September 8, 2013

Abstract

Chapter 1

Introduction

The goal of this thesis is to study and better understand the dynamics of particles in flows, and is a continuation of two previous masters theses [1][6]. This is done by analysing micrometer length glass particles in a shear flow and comparing this to theoretical models. Before discussing either of these processes more in depth some background and basic theory is needed.

1.0.1 Background

The study of particle dynamics in flow began with Einsteins paper from 1905 [4] in which he showed that the viscocity of suspended particles would increase the viscocity of the fluid and how much. Jefferey in his 1922 paper [7] extended these results to ellipsoidal axis-symmetrical particles but then also studied the orientational dynamics of the particles. Disregarding intertial effects the motion was found to be periodic and depending only on the initial condition of the particle.

Development of tri-axial particle, started with Gierszewski & Chaffey (1978)[5] and was continued by Hint & Leal (1979) and more recently by Yarin et al in 1993[2]. Now the dynamics found for axis-symmetric particles by Jeffrey were periodic, but it was shown first by Hinch & Leal that some orbits would be doubly periodic, in other words following two separate independent periods. Yarin then was able to use numerical simulations to generate a surface of section [8] for some relations between the two minor axes showing that not only was there double periodic or quasi periodic orbits but for sufficiently large differences in axes there would be chaotic orbits. Several other surfaces of were also produced by Johansson (2012)[1] with higher resolution thanks to improvements in computing power. It was there shown that only very small asymetries on the order of 1% will lead to quasi-periodic motion for some initial conditions.

The experimental history of verifying these results is more sparse,

The most extensive work on tri-axial particles was done by Hinch & Leal in their 1979 paper [3]

The dynamics of particles in flow has been studied for many years, with early contributions from Einstein in his 1905 paper "Something something Einstein paper"[**?**], continued by Whatever his name is Jeffrey in 1922 and many since. Jeffrey derived analytically explicit solutions for the motions of triaxial particles in a shear flow called 'Jeffrey Orbits' (see section **??**) which have been used in various theoretical developments. However there is rather limited experimental evidence that such orbits actually exist [**?**]. Previous work by Einarsson[**?**] et al did not satisfactorly show this, presumably because of assymetric particles, possible thermal noise and inaccurate tracking. This thesis has used particles with better symmetry and bla bla bla

A very simple description of the experimental setup is a microfluidic channel where the rotational dynamics of microrods are captured using a camera connected to a confocal microscope. A more detailed description can be found in section **??**.

The focus of this thesis is on improving the experimental setup both in terms of the quality of results as well as the efficiency and ease of gathering such results

as well as evaluating the results of these improvements.

The main improvements have been to replace the particles as well as automating the tracking of particles and the flow direction in the channel.

1.1 Background

1.2 Experimental Setup

In order to study the dynamics of particles, a channel made from PDMS and bonded onto a glass slide. A fluid containing the traxial glass particles that can be seen in fig re REF HERE is pumped at a constant rate through the channel using a INSERT THE PUMP NAME HERE. To observe the particles, the channel is placed upon a confocal microscope connected to a INSERT CAMERA MODEL HERE. The channel is then moved using a INSERT STEP ENINE NAME HERE controlled from a computer. A mroe detailed description of the setup can be seen in figure REF to SETUP IMAGE THAT I MAKE

1.2.1 The particles

Previously the particles used in the experiment were polymeric made by swirling an apoxy solution in a vortex. This produces rod like particles of different lengths, but very often included noticeable defects such as being bent, small lumps etc. To improve results glass particles from Nippon Glass company in Japan were brought in. As they are mainly manufactured to serve as spacing rods in LCD screens they have a very well determined width but then broken at varying lengths. These breaking points are the only real visible point of imperfection of the rods. The specification of length and width can be seen in figure ??

While the glass rods are far more regular in terms of size and shape, they do have on major problem. The density of the glass is 2.57 g/cm^3, significantly higher than water which has a density of around ENSITY OF WATER at 20 degrees C and glycerol which has a density of DENSITY OF GLYCEROL. And so the particles will sink very quickly in any mix of water and glycerol.

The solution is to use Sodium Metatungstate, water soluble mineral which gives the resulting mix a maximum density of around DENSITY OF SOMT which is more than sufficient to keep the particles suspended. It is however not without its own issues which will be discussed in the discussion portion of the thesis.

First the viscosity of the mix is significantly lower than the glycerol and water mix used previously (a 1:4 mix of glycerol and water was commonly used) which means the system is more sensitive to noise. Second the density of the solution changes when the water mixed in evaporates. As the ratio of water to mineral is relatively high, clearly more than 1:1 by weight, a small percentage of water evaporating will result in significant change in density

1.2.2 Sodium Metatungstate

I guess we use sodium meta tungstate. But does this really need a whole section? Seems like overdoing it... but what THE EQUATION FOR MODIFYING VISCOCITY

$$\rho_a = \frac{m_a}{V_a} = \frac{V_b \rho_b + V_{mix} \rho_{mix}}{V_b + V_{mix}} \tag{1.1}$$

So if we want to find V_{mix} we get

$$V_{mix} = \frac{V_b (\rho_b - \rho_a)}{\rho_a - \rho_{mix}} \tag{1.2}$$

Chapter 2

Theory

In order to better understand the results and discussions in this thesis some rather basic results in fluid dynamics, image analysis and other fields need to be discussed. It is however not the focus of this thesis and as such I will try to be as brief as possible, and an experienced reader can safely skip to the next chapter.

2.1 Fluid Dynamics

In order to understand the limitations and behaviours of the experiment we need to know about a few key concepts in fluid dynamics.

2.1.1 Reynold's Number

The Reynolds number (Re) is a dimensionless number describing the ratio of intertial forces to viscous forces in a flow. This is not a very strict definition, but suffices to explain that the Reynolds number can be used to characterize the so called flow regime of a system.

There are two major types of flows, Laminar flow and turbulent flow, sometimes also talking about transitional flow being the region between the two but it is not of great importance to this thesis.

Laminar flow. nonturbulent streamline flow in parallel layers. There are no cross currents perpendicular to the direction of the flow, which in this experiment is relatively straight forward. An example of a laminar flow profile can be seen in figure 2.1.1 as well as turbulent flow. Essentially laminar flow is the regime where the viscous forces are larger than the intertial forces.

Turbulent flow is characterized by violent, unsteady and unpredictable flow. This is the regime where the intertial forces are larger than the viscous forces.

The Reynolds number is the primary tool used to describe the regime of a flow, and while there is no clear number at which a flow stops being laminar but the value usually used is that the flow is laminar if $Re << 1$

Turbulent

Laminar
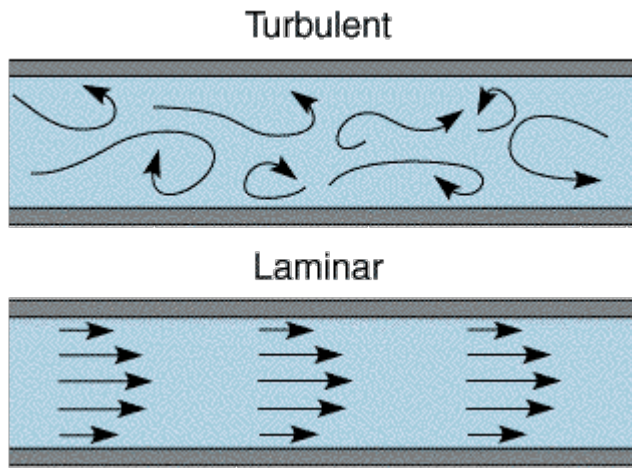
2.1.2 Stokes Drag and Stokes law

Stokes Law:

$$v_s = \frac{2}{9}\frac{\delta\rho}{\mu}gR^2 \tag{2.1}$$

$\delta\rho = 0.01 \ ... \ 0.001$
$\mu = 8 * 10^-3$
$g = 9.82$
$R = 5 - 35 \cdot 10^-6$

2.2 Jeffrey Orbits

2.3 Kalman filter

Chapter 3

Automated Tracking

TODO: READ UP ON THE EFFICIENCY OF THE CANNY EDGE DETEC-
TION TAKE AN IMAGE OF THE STATIC NOISE REDUCTION (DOES
IT ACTUALLY WORK?!) GET AN IMAGE OF BEFORE AND AFTER
SMOOTHING, PREFERABLY INCLUDE A CANNY EDGE DETECTION
OF BOTH ADD ANTONS THESSIS TO BIBLIOGRAPHY WORK MORE
ON KALMAN FILTER SECTION WRITE ABOUT THE TIME IT TAKES
TO DO VARIOUS STUFFS

3.1   Noise Reduction

The first step in tracking a particle is to correctly identify it in the image given.
To do this we want to eliminate as much noise from the image as we can. The
first type of noise we will eliminate is static noise, this is noise present in every
image and results from dirt or scratches on the lens of the camera or microscope.
The easiest solution to such noise would of course be to clean the instruments,
but despite numerous attempts of carefully cleaning every surface a noticeable
of static noise would always remain.

   This means one must use algorithmic noise reduction methods to remove
this noise. The method employed is a simple averaging that takes N pictures
at different positions in the channel to generate an average image where any
particular features of the channel would disappear and only the static noise
remain. This can be seen in figure STATIC NOISE REDUCTION IMAGE,

   The second form of noise eliminated are objects of no interst, such as the
lines in the PDMS channel, from the scratches made polishing the cast the
channel is molded from. Or, possible dirt on the cover glass. To reduce this
noise, the image is blurred with a gaussian blur filter of size 7 with $\sigma = 1$. THE
RESULTS OF SMOOTHING CAN BE SEEN IN ANOTHER IMAGE

3.2 Canny Edge Detection

The Canny Edge invented by John Canny in his 2011 paper the canny of cane [**?**]detection is generally considered the most advanced and best performing edge detection of the simple filter functions. Without going in to the finer details, given an image matrix **I** where each value corresponds to the light intensity $i_{x,y}$ of that pixel at index x, y the Canny edge detector will try to find the cohesive pixels $E = \{e_1, e_2...e_n\}$ where there is a noticeable change in intensity. In other words, what we call an "edge" an image.

This is accomplished in two steps. First a Sobel Filter edge image is computed by looking at the change in intensity at every pixel from 3 possible directions and averaging these.

S = MATHEMATICS OF SOBEL

We then consider a Then, a pixel

$p_{x,y} \in E$ if $S(x,y) > T_{high}$

where T_{high} is a predetermined threshold value.

Secondly we recursively check all pixels neighbouring an edge

MATH?

if they are higher than some threshold value T_low. if they are, they are also considered part of the edge. This is repeated until no more pixels are added. An image illustrating this process can be seen in figure FIG. The benefit of the Canny edge detection over the simpler Sobel is that it is much easier to detect cohesive objects that vary in intensity without getting a lot of other noise in the image. The only real drawback of the Canny Edge detection is the computation time, and thus the implementation from the Open Computer Vision (OCV) was used, as this is a heavily optimized routine written in C++ with real time uses in mind. Thanks to this the computing for the Canny Edge of a 260x260 Image takes about X ms and thus is of little importance in the overall time per frame.

After noise reduction the Canny Edge Detection is used to find the most significant edges in the image.

3.3 Contour detection and selection

Once an edge image has been generated, the OCV package has another useful function, `Contours` which returns a list of every contiguous group of edge pixels. If we have chosen the threshold values to the edge detection correctly, this should include the particle or a good approximation of it.

In order to find the correct contour, a few techniques are used to find the correct contour.

First particles whose total size is less than some minimum value, n_{min} or larger than some maximum value n_{max} are ignored. Then the position pP_i of each contour $C_i = p_1, p_2...p_n$ is calculated as the average pixel position

$$P_i = \sum_{j}^{n} p_j/n$$

9

This position is compared to the expected position of the Kalman filter, which the very first frame is the middle position.

Finally a 'thinness value' is calculated according to eq 3.1

$$w_{thin} \left(\frac{n}{d_{max}^2} \right)^2 \tag{3.1}$$

. where w_{thin} is a weighting constant, n is the number of pixels in the contour and d_{max} is the longest distance between two pixels in the where I am not really sure I should do this now that I have so few particles, but I do it none the less!

3.4   Kalman Filter

When the particle is at constant motion in the channel the equations of motion give us

$$\begin{bmatrix} x_n \\ v_{x,n} \\ y_n \\ v_{y,n} \end{bmatrix} = \begin{bmatrix} x_{n-1} & +v_{x,n-1} \\ v_{x,n-1} & \dots \\ y_{n-1} & +v_{y,n-1} \\ v_{y,n-1} & \end{bmatrix} + \begin{bmatrix} 0 \\ c_{xn} \\ 0 \\ c_{yn} \end{bmatrix} y_n v_{yn} \tag{3.2}$$

We can rewrite this in matrix form as

$$\begin{bmatrix} x_n \\ v_{x,n} \\ y_n \\ v_{y,n} \end{bmatrix} = \begin{bmatrix} 1 & \Delta t & 0 & 0 \\ 0 & 1 & 0 & 0 \\ 0 & 0 & 1 & \Delta t \\ 0 & 0 & 0 & 1 \end{bmatrix} \cdot \begin{bmatrix} x_{n-1} \\ v_{x,n-1} \\ y_{n-1} \\ v_{y,n-1} \end{bmatrix} + \begin{bmatrix} 0 & 0 & 0 & 0 \\ 0 & 1 & 0 & 0 \\ 0 & 0 & 0 & 0 \\ 0 & 0 & 0 & 1 \end{bmatrix} \cdot \begin{bmatrix} 0 \\ c_{x,n-1} \\ 0 \\ c_{y,n-1} \end{bmatrix} \tag{3.3}$$

Now if we want to transform this to the measured data we have to simply multiply by a constant pixel-to-meter constant, which has been meassured to be around $1/940 = 1.06 \cdot 10^{-3}$

$$Q = \begin{bmatrix} 0 & 0 & 0 & 0 \\ 0 & 1 & 0 & 0 \\ 0 & 0 & 0 & 0 \\ 0 & 0 & 0 & 1 \end{bmatrix} \tag{3.4}$$

Which we can easily re-write as a Kalman filter

$$\hat{\mathbf{x}}_n = \mathbf{A}_n \mathbf{x}_{n-1} + \mathbf{B}_n \mathbf{u}_n + \mathbf{w}_n \tag{3.5}$$

$$\hat{\mathbf{P}}_n = \mathbf{F}_n \mathbf{P}_{n-1} \mathbf{F}_n^T + \mathbf{Q}_n \tag{3.6}$$

with

$$\mathbf{x}_n = [x_n v_{x,n} y_n v_{y,n}]^T \tag{3.7}$$

$$\mathbf{A} = \begin{bmatrix} 1 & \Delta t & 0 & 0 \\ 0 & 1 & 0 & 0 \\ 0 & 0 & 1 & \Delta t \\ 0 & 0 & 0 & 1 \end{bmatrix} \tag{3.8}$$

$$\mathbf{B}_n = \begin{bmatrix} 0 & 0 & 0 & 0 \\ 0 & 1 & 0 & 0 \\ 0 & 0 & 0 & 0 \\ 0 & 0 & 0 & 1 \end{bmatrix} \tag{3.9}$$

$$\mathbf{u}_n = \begin{bmatrix} 0 \\ c_{x,n-1} \\ 0 \\ c_{y,n-1} \end{bmatrix} \tag{3.10}$$

and we add the update part as

$$\mathbf{K}_n = \hat{\mathbf{P}}_n \mathbf{H}_n^T (\mathbf{H}_n \hat{\mathbf{P}}_n \mathbf{H}_n^T) \tag{3.11}$$

$$\mathbf{x_n} = \hat{\mathbf{x}}_n + \mathbf{K}_n (\mathbf{y} - \mathbf{H}_n \hat{\mathbf{x}}_n) \tag{3.12}$$

$$\mathbf{P} = (\mathbf{I} - \mathbf{K}_n \mathbf{H}_n) \hat{\mathbf{P}}_n \tag{3.13}$$

3.5 Stabilizing the tracking

Once a state estimation has been made, we want to adjust the speed of the step engine to, as best as possible, match that of the particle. This is done by looking both the position and velocity of the particle and going through the conditional statements shown in figure CONDITIONAL CORRECTION VECTOR.

The goal is to limit the amount of corrections made, as changing the velocity is rather time intensive as discussed in section 3.6, as well as keeping the particle stable. There is also no point in trying to completely eliminate movement

3.6 Time Considerations

A higher FPS will allow the particle detection to be better, improve the position saving and allow the particle tracking to be more stable as well. So maximizing the FPS, ie reducing the computational time of each task, is a clear goal for a good automated tracking. A list of the different tasks and their average execution times can be seen in table 3.6

Task	Average time	Std deviation
Capture screen	1000	200
Find edges	200	20

We can clearly see that FPS is limited primarily by three routines: The screen capture routine, the change velocity routine and finally the save position routine. The first and last are unavoidable and must be done every frame by definition if we are interested in knowing the particles position as well as possible. This means we simply want to use the velocity correction as little as possible. Since the time constraint is in the communication with the step engine, there is not any optimization to be done here, at least not within the scope is this thesis.

Chapter 4

Experimental Setup

Chapter 5

Results

Chapter 6

Discussion

Appendix A

Raw data

Bibliography

[1] Johansson A. Analysis of empirical data on the tumbling of microrods in a shear flow. Master's thesis, Chalmers Univeristy of Technology.

[2] I. V. ROISMAN A. L. YARIN, O. GOTTLIEB. Chaotic rotation of triaxial ellipsoids in simple shear flow. *J. Fluid Mech*, vol 340:83–100, 1997.

[3] L. G. Leal E. J. Hinch. Rotation of small non-axissymmetrical particles in a simple shear flow. *J. Fluid Mech*, 92:591–608, 1979.

[4] Albert Einstein. A new determination of molecular dimensions. *Annalen der Physik*.

[5] Paul J. Gierszewski and Charles E. Chaffey. Rotation of an isolated triaxial ellipsoid suspended in slow viscous flow. *Canadian Journal of Physics*, 56(1):6–11, 1978.

[6] Einarsson J. Low reynolds number particle dynamics. Master's thesis, Chalmers Univeristy of Technology.

[7] G. B. Jeffrey. The motion of ellipsoidal particles immersed in a viscous fluid. *Proceedings of the Royal Society A*, 102.

[8] Frank C. van den Bosch. lecture 1: Surfaces of section. Online material for course.